iScience

CellPress
OPEN ACCESS

Article

Coupling relationships between urban block spatial morphology and microclimate in severe cold regions

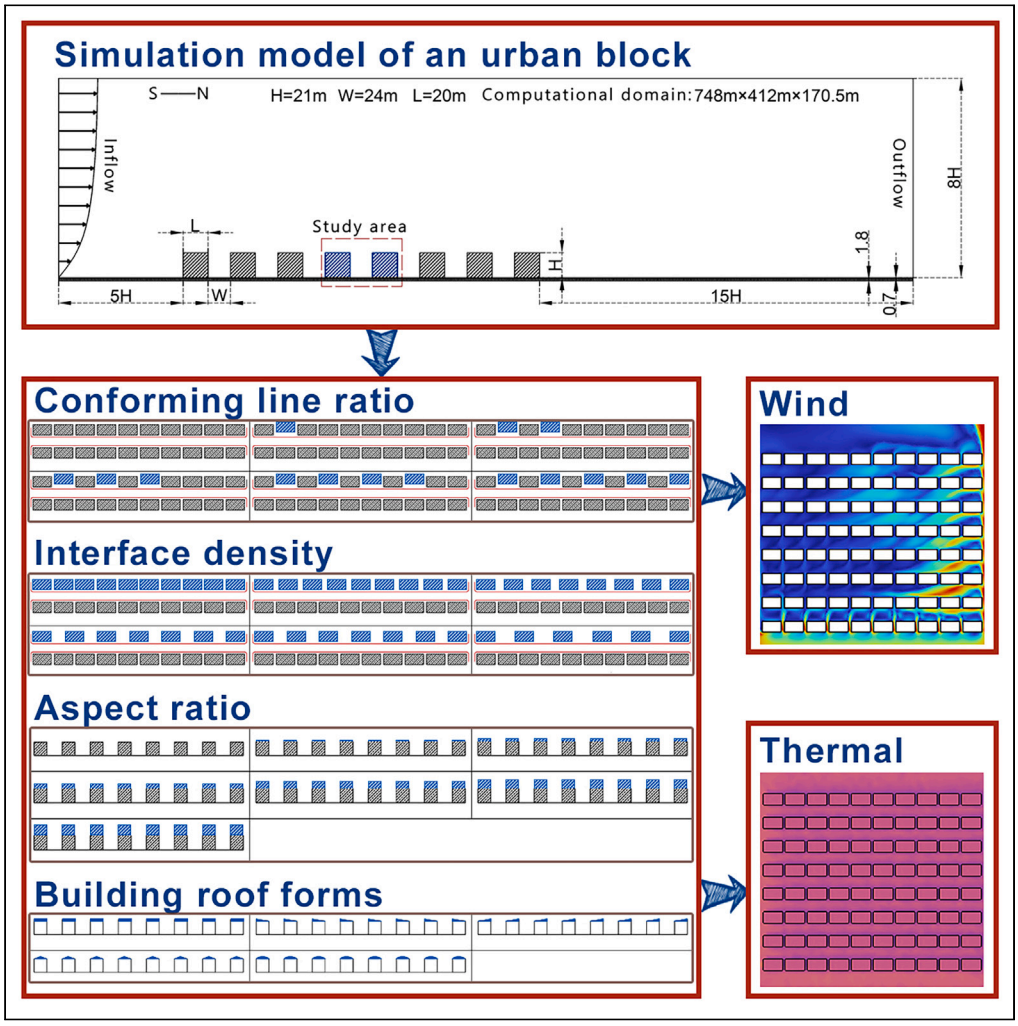

Guang Zhu, Yun Chen, Wen Wu, Ruihan Liu, Yu Tang, Pengcheng Li, Aowei Xu

wuwen@mail.neu.edu.cn

Highlights

Explored the influence of spatial morphology on microclimate using numerical simulation

The impact of spatial morphology on microclimatic conditions is both evident and varied

Proposed spatial layout design strategies for various streets in severe cold regions

Zhu et al., iScience 26, 108313
November 17, 2023
https://doi.org/10.1016/j.isci.2023.108313

iScience

CellPress
OPEN ACCESS

Article

Coupling relationships between urban block spatial morphology and microclimate in severe cold regions

Guang Zhu,[1] Yun Chen,[1] Wen Wu,[1,3,*] Ruihan Liu,[1] Yu Tang,[1] Pengcheng Li,[1] and Aowei Xu[2]

SUMMARY

This study investigates the relationship between urban block spatial morphology and microclimate in severe cold regions, using Shenyang, China as a case study. We employed computational fluid dynamics theory-based numerical simulation software and a controlled variable approach to analyze the microclimate effects of four key aspects: street conforming line ratio, street interface density, street aspect ratio, and building roof forms. The primary findings are as follows: Decreasing conforming line ratios initially increase average wind speed and temperature. Lower interface densities reduce average wind speed but raise temperature. Higher aspect ratios correspond to increased wind speed and decreased temperature. Additionally, upward sloping roofs correlate with higher average wind speed and temperature. This research provides a perspective for evaluating urban microclimates, considering human perception of urban block space. It also suggests spatial layout design strategies for different types of streets in severe cold regions, considering the climate environment.

INTRODUCTION

The unprecedented global urbanization process has led to a substantial influx of individuals into cities, particularly in China, where the urban population has grown by 36.5% from 2000 to 2021. Correspondingly, the total population residing in urban areas grew by 1.31 times, accompanied by a 2.01 times expansion of the urban built-up area.[1] Despite covering a small fraction of the Earth's land surface, urban areas accommodate over half of the world's population.[2] The rapid progression of urbanization has resulted in the intensification of the urban heat island effect, as natural environments are gradually replaced by urban settings. The urban climate, influenced by macroclimate conditions and urban morphology, represents a dynamic and intricate system that significantly impacts human comfort and outdoor space utilization.[3] Consequently, comprehending the implications of urbanization on urban climate has become a subject of great interest in the scientific community.[4–7]

Urban climate exhibits diverse characteristics and can be studied from three perspectives: mesoscale, local scale, and microscale.[8,9] Mesoscale urban climate research examines environmental conditions within a range of 10–100 km, while investigations of local-scale urban climate focus on a range of 1–10 km.[10,11] In contrast, microscale urban climate studies encompass a smaller range of approximately 2 km, closer to the scale of buildings, thereby magnifying the influence of buildings on the urban microclimate.[12–14]

Since the 1970s, with the emergence of the concept of sustainable development and advancements in urban microclimate research, scholars have established a correlation between urban built environments, microclimate, and spatial morphology.[15,16] Moreover, it has been demonstrated that spatial morphology within urban blocks plays a significant role in influencing microclimate.[17,18] ENVI-met simulation experiments have revealed that street aspect ratio and sky view factor (SVF) have a notable impact on the thermal environment within urban blocks. Deeper streets, higher aspect ratios, and lower SVF contribute to reducing the average radiant temperature within streets.[17,19] Additionally, factors such as windward area ratio of buildings within streets,[20–22] variations in building height,[23–25] street conforming line ratio, and building geometric characteristics (e.g., roof forms, balconies, facade design)[26–30] also influence the climate dynamics within urban blocks.

However, current microscale climate studies on urban blocks predominantly focus on individual climatic factors such as wind or thermal environment, limiting their ability to capture the comprehensive variations of microclimate within blocks. Furthermore, the selection of spatial morphology indicators for urban blocks remains relatively limited, failing to holistically consider these indicators. Consequently, existing research outcomes do not fully accommodate the complexity and diversity of spatial layouts in urban block design.[31,32] This study aims to explore the influence of different indicator parameters of urban block spatial morphology on microclimate through numerical modeling. Specifically, it simulates the distribution of microclimate within urban blocks based on four morphology indicators related to spatial morphology: street conforming line ratio, interface density, aspect ratio, and roof forms. The objective is to provide urban designers with essential references and evaluation criteria during the early stages of design, enabling the formulation of more scientifically grounded planning strategies.

[1]JangHo Architecture College, Liaoning Provincial Key Laboratory of Urban and Architectural Digital Technology, Northeastern University, Shenyang 110819, China
[2]Key Laboratory of Forest Tree Genetics, Breeding and Cultivation of Liaoning Province, College of Forestry, Shenyang Agricultural University, Shenyang 110866, China
[3]Lead contact
*Correspondence: wuwen@mail.neu.edu.cn
https://doi.org/10.1016/j.isci.2023.108313

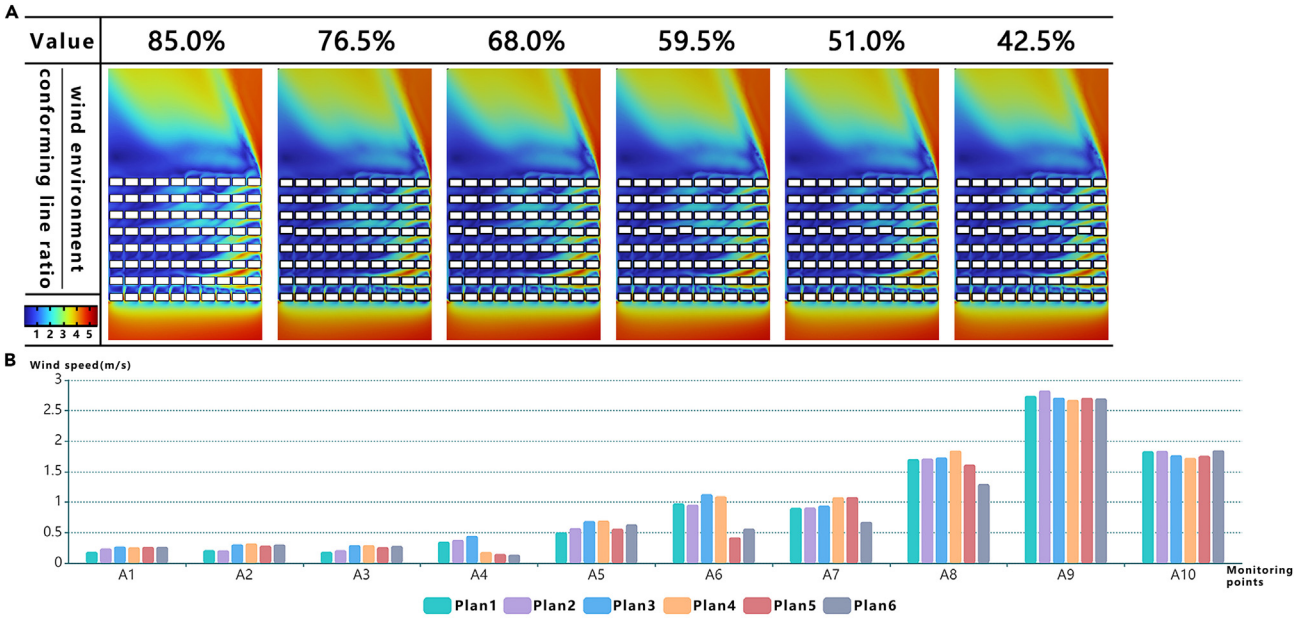

Figure 1. Simulation results of street wind environment under different conforming line ratio parameters

(A) Visualization of the simulated street wind environment.

(B) Wind speed at each monitoring point within the street.

This endeavor will contribute to establishing a favorable urban microclimate environment and enhancing the level of sustainable development for human habitation.[33,34]

RESULTS

Simulation results of street conforming line ratio

The simulation results of the street conforming line ratio (Figure 1) show that there are no significant variations in wind speed at measurement points A1–A3, which are located farther away from the street canyon inlet and within the wind shadow area. However, it is observed that the wind speed at each measurement point is higher in the simulated conditions of the plan 3 and plan 4 models compared to the other models. This suggests that when the street conforming line ratio falls within the range of 59.5%–68%, the wind speeds within the urban street canyon are noticeably enhanced, promoting better ventilation and air quality renewal.

Based on the thermal environment simulation results (Figure 2), it is evident that the temperature measured at measurement point A1 consistently exceeds that of other measurement points across various plans models. This finding can be attributed to the distance of A1 from the air inlet of the street, as depicted in Figure 1, where the wind speed is relatively low. The reduced wind flow facilitates heat accumulation, leading to elevated temperatures at A1. With the exception of plan 6 model, the temperature differences among measurement points are not significant under the other models. This suggests that a low street conforming line ratio (42.5%) induces instability in the internal temperature within the street canyon.

Simulation results of street interface density

The analysis of the wind environment simulation results (Figure 3) reveals that plan 1 and plan 6 models exhibit similar effects on the wind environment in terms of interface density. Notably, in the eastern half of the street, specifically at measurement points A6 to A10, both plan 1 and plan 6 models demonstrate higher wind speeds compared to the other models. At measurement points A1 to A3, as the interface density decreases, the wind speed initially increases and then decreases. Conversely, at measurement points A4 to A10, the trend is reversed, with the wind speed decreasing initially and then increasing as the interface density decreases.

The analysis of the thermal environment simulation results (Figure 4) highlights the impact of street interface density on temperature distribution. It is evident that temperature tends to accumulate on the western side of the street, particularly at measurement point A1, where the highest temperature is observed. In contrast, there is minimal temperature variation at the two measurement points A1 and A10 across the different models, while significant variations are observed at other measurement points. This indicates that changes in interface density lead to shifts in the positions of buildings along the street, resulting in temperature fluctuations. Among the tested models, plan 3 exhibits the smallest range of temperature fluctuations at each measurement point within the street, whereas plan 6 shows the greatest fluctuation range. Notably, measurement point A5 in plan 4 records the lowest temperature.

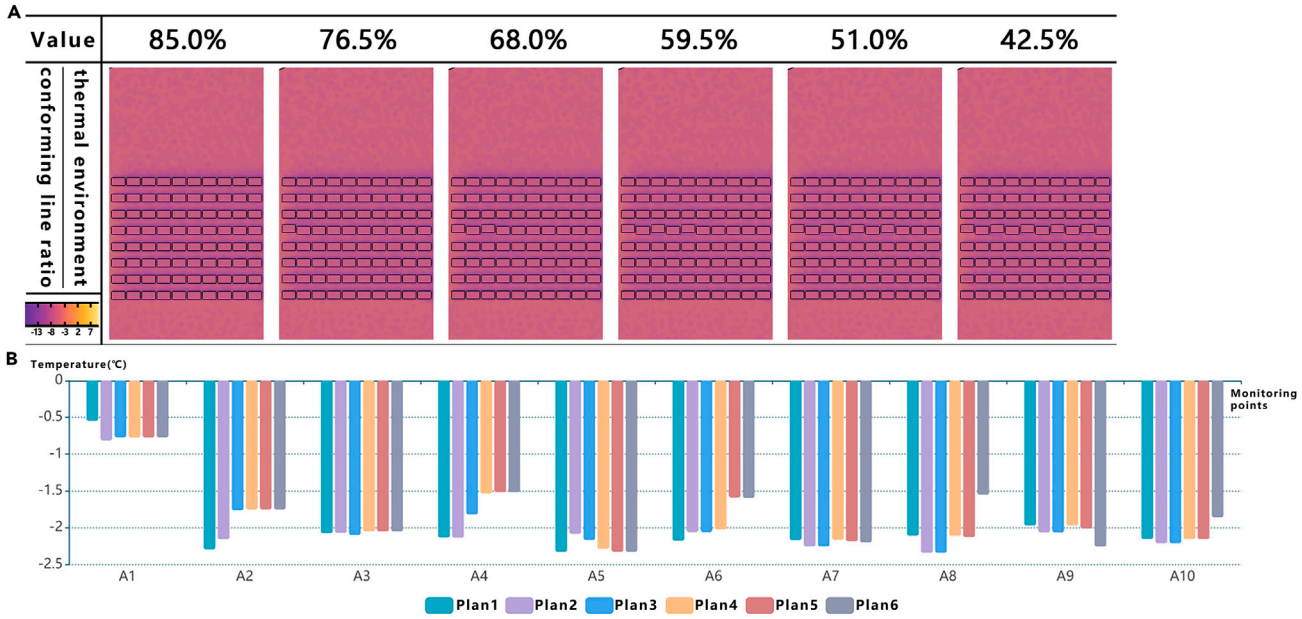

Figure 2. Simulation results of street thermal environment under different conforming line ratio parameters

(A) Visualization of the simulated street thermal environment.

(B) Temperatures speed at each monitoring point within the street.

Simulation results of street aspect ratio

When analyzing the wind environment simulation results (Figure 5), in relation to the street's aspect ratio, several observations can be made. Firstly, the models from plan 1 to plan 6, there is minimal difference in wind speed at measurement points A1 to A3 within the street. These measurement points are situated in the wind shadow areas of the street, indicating that changes in the street aspect ratio have limited impact on the wind environment in these regions. Secondly, as the street aspect ratio increases from plan 1 to plan 7 models, the wind speed data at measurement points A4 to A6 initially decrease and then increase, while the data at measurement points A7 to A8 gradually increase. Conversely, the data at measurement point A9 decrease gradually, and at measurement point A10, they stabilize. These findings suggest the formation of vortices near measurement point A8 within the street, which become more pronounced with an increase in the street aspect ratio. As a result, significant variations in the wind environment occur. Overall, the simulation results demonstrate that changes in the aspect ratio of the street can have a notable impact on the wind environment, particularly in the vicinity of measurement point A8, where the formation of vortices is observed.

The thermal environment simulation results (Figure 6) reveal the influence of the street's aspect ratio on temperature distribution within the street. As the aspect ratio increases, there is a gradual rise in temperatures at measurement points A1 to A2, which are located within the wind shadow areas of the street. This observation, combined with the wind environment analysis depicted in Figure 5, suggests that an increased aspect ratio contributes to heat accumulation within these wind shadow regions, leading to a thermal insulation effect. On the other hand, for measurement points A3 to A10, an overall decreasing trend in temperatures within the street is observed as the street aspect ratio continues to increase. This indicates a negative correlation between temperature and the street aspect ratio in the non-wind shadow areas of the street. These findings highlight the complex interplay between the street's aspect ratio and temperature distribution, with distinct thermal patterns emerging in different regions of the street.

Simulation results of roof forms of buildings along the street

The simulation results of the wind environment (Figure 7) demonstrate the significant impact of the roof forms of buildings along the street on the wind speed within the street. The wind speed follows a specific order: upward sloping roof > flat roof > downward sloping roof. The difference in wind speed between the round roof and triangular roof forms is not pronounced, falling between the values observed for upward sloping roofs and flat roofs. This suggests that the form of building roofs can modify the distribution of the flow field above the buildings, thereby influencing the wind environment within the street. Additionally, under prevailing winds from the southeast-south during the winter season in Shenyang, when the inclination angle of the building roof form tends toward an upward slope, the wind speed within the street also increases accordingly. These findings highlight the importance of considering the design and form of building roofs in urban planning to optimize the wind environment and enhance ventilation within street canyons.

The forms of building roofs also play a significant role in shaping the thermal environment within the street (Figure 8). Specifically, during the winter season in Shenyang, the upward sloping roof exhibits a more pronounced effect in maintaining and elevating the air temperature within the street. The flat roof follows in terms of thermal performance, while the downward sloping roof demonstrates the poorest performance. On

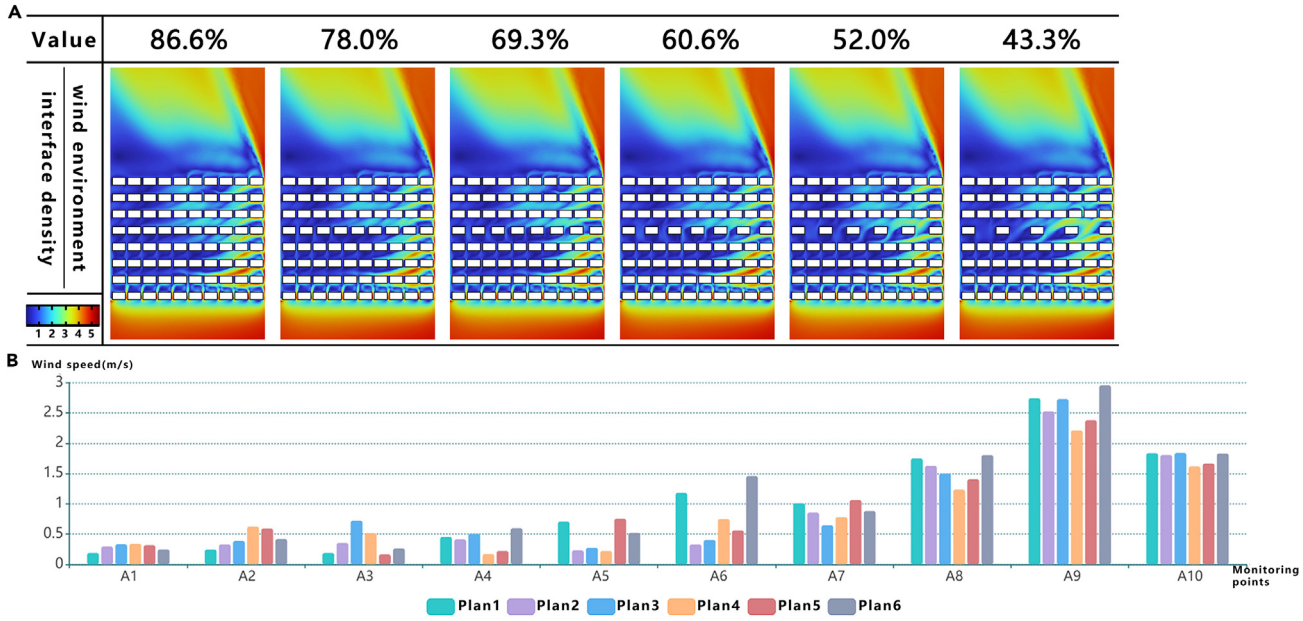

Figure 3. Simulation results of street wind environment under different interface density parameters

(A) Visualization of the simulated street wind environment.

(B) Wind speed at each monitoring point within the street.

average, there is a temperature difference of nearly 5°C between the most optimal and the poorest performing roof forms. This observation aligns with the influence of building roof forms on the wind environment. The upward sloping roof shows the most favorable effects on ventilation and thermal insulation within the street, while the downward sloping roof performs poorly in both ventilation and thermal insulation aspects.

These findings emphasize the importance of considering the design and form of building roofs not only for optimizing the wind environment but also for enhancing thermal comfort and energy efficiency within street canyons. Proper roof forms can contribute to better temperature regulation and insulation, leading to improved urban microclimate conditions.

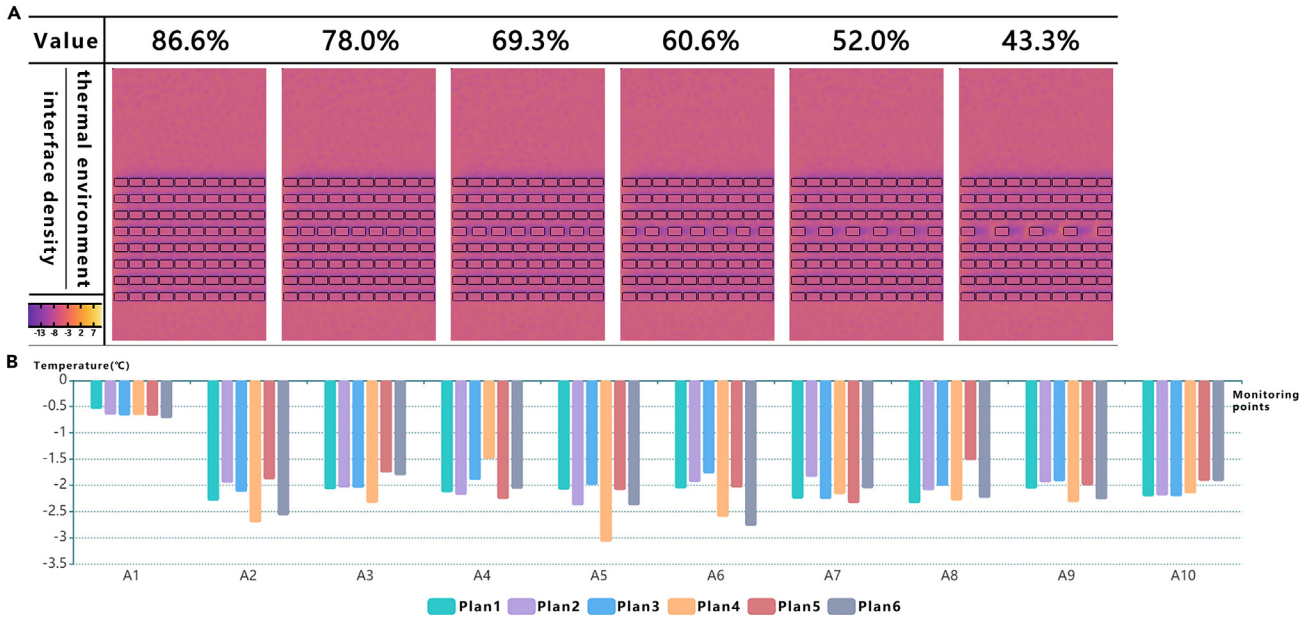

Figure 4. Simulation results of street thermal environment under different interface density parameters

(A) Visualization of the simulated street thermal environment.

(B) Temperatures speed at each monitoring point within the street.

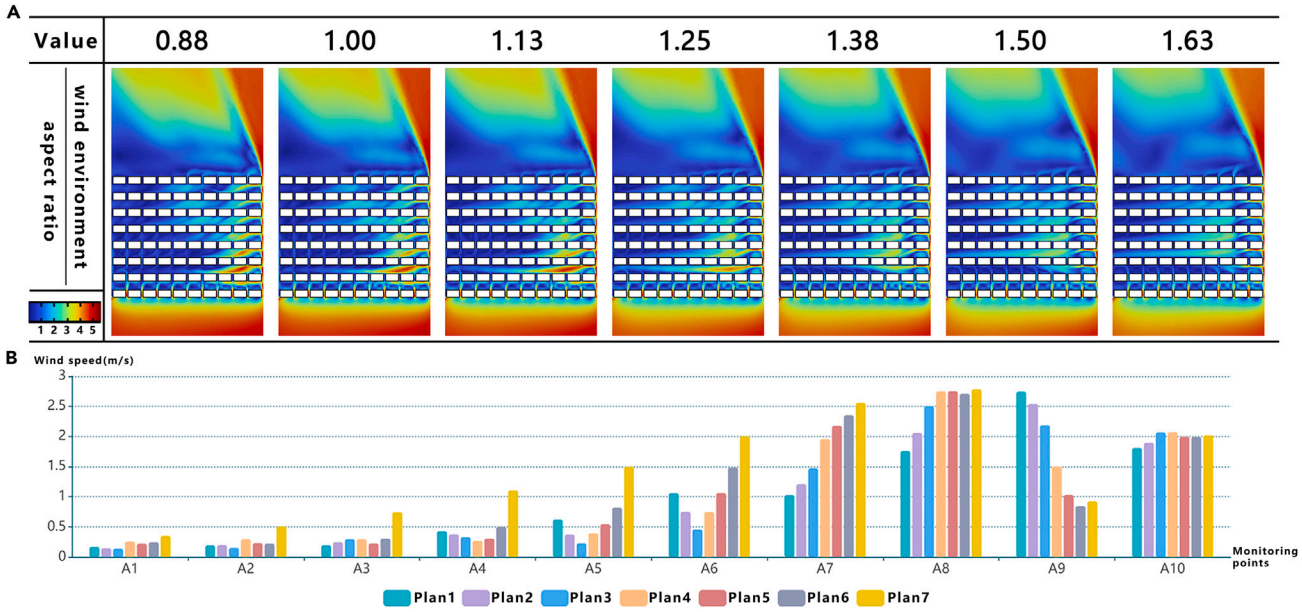

Figure 5. Simulation results of street wind environment under different aspect ratio parameters

(A) Visualization of the simulated street wind environment.

(B) Wind speed at each monitoring point within the street.

DISCUSSION

Block space perception under quantitative analysis

In line with Lynch's concept of "The Image of the City,"[35] the perception of urban block spaces involves a reciprocal relationship between observers and the observed environment. While studying the physical characteristics of urban block spaces, it is crucial to consider individuals' cognitive mechanisms regarding the streets within the blocks.

Many studies in the literature found that street conforming line ratio, interface density, aspect ratio, and building roof forms are essential in creating a pleasant microclimate and thermal comfort in an urban canyon under different climate conditions. The street conforming line ratio (B/P) serves as an indicator of the continuity of street walls, where higher values indicate stronger continuity.[25] Public preference studies suggest that B/P values ranging from 50% to 90% contribute to the creation of continuous and well-structured physical interfaces with subtle spatial variations. The optimal range falls between 50% and 70%.[24]

The street interface density (De) quantitatively analyzes the density of interfaces in the horizontal dimension of streets, and higher values enhance spatial perception.[36] Analyzing statistical data from Alan Jacobs' book "Great Streets,"[37] artificially planned streets tend to have interface densities of approximately 72%–83%, while naturally evolved streets exhibit densities around 86%–92%. Research concludes that an interface density of 70% or above is a necessary condition for creating excellent street spaces.[1]

The street aspect ratio (H/D) characterizes the vertical form of street interfaces. Studies by Camillo Sitte[38] and Alan Jacobs[39] have established a close relationship between H/D values and the spatial perception of streets. They propose that an H/D value between 1 and 1/2 is most appropriate, while $H/D \leq 1/2$ creates a sense of openness and distance, and $H/D > 1$ generates a sense of enclosure and compression.

Based on a comprehensive analysis of these three indicators, the perceived quality of block spaces can be categorized into three levels: excellent, good, and poor, as shown in Table 1.

Street microclimate analysis under different spatial morphological indicators

To gain a deeper understanding of the street microclimate, average wind speed, average temperature, and variance calculations are performed for measurement points A1 to A10 within the street canyon. By fitting a variance curve, a more systematic evaluation of the variations in street microclimate under different spatial morphological indicators can be achieved. This analytical approach enables the quantification of microclimate changes within the street canyon, providing quantitative data on average wind speed, average temperature, and variance. The variance fitting curve unveils the influence of various spatial morphological indicators on the street microclimate, enabling an assessment of the magnitude and trends of their impact.

The relationship between the street conforming line ratio and the microclimate within the street canyon is elucidated (Figure 9). Comparing the average values of the measurement data across different plans' models, it is evident that as the street conforming line ratio decreases, the average wind speed initially increases and then decreases, while the average temperature within the street gradually rises. The variance fitting curve demonstrates that as the street conforming line ratio decreases, the variance values for both wind speed

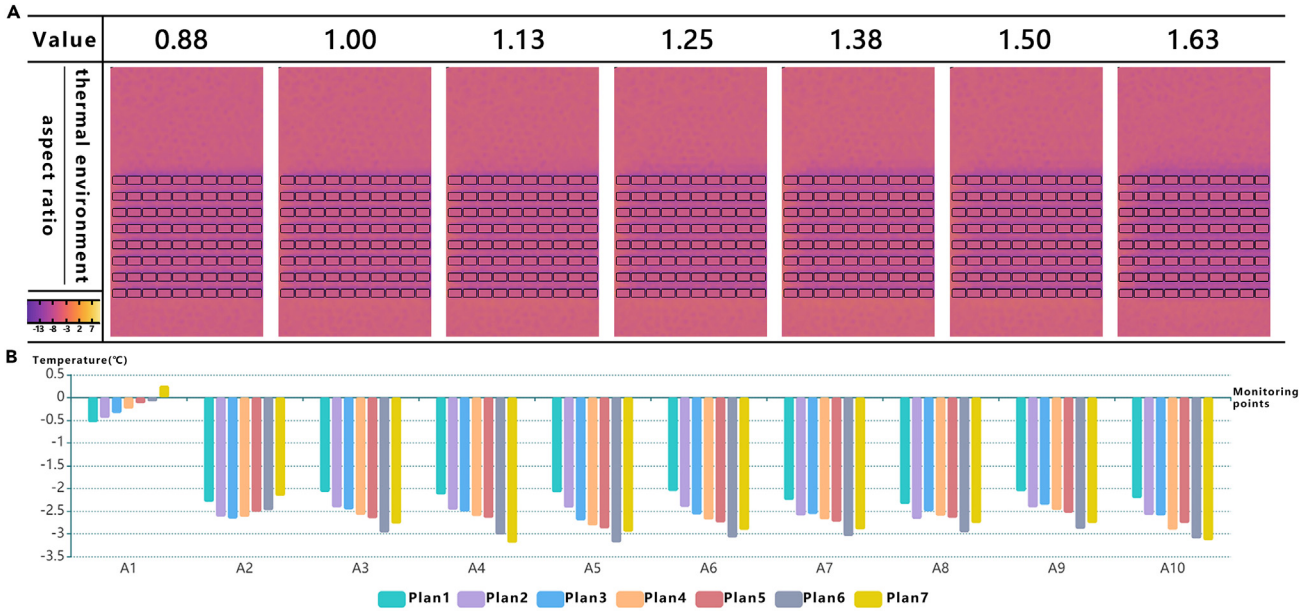

Figure 6. Simulation results of street thermal environment under different aspect ratio parameters

(A) Visualization of the simulated street thermal environment.

(B) Temperatures speed at each monitoring point within the street.

and temperature measurements initially decrease and then increase. However, the magnitude of these changes is not substantial across different plans' models of street conforming line ratio, suggesting that variations in street conforming line ratio do not result in significant fluctuations in the street microclimate. Therefore, when selecting the street conforming line ratio for urban streets, a moderate value may be preferable if ventilation is a priority, as seen in plan 3 or plan 4. Alternatively, a lower street conforming line ratio, such as plan 5 or plan 6, may be favored for emphasizing thermal insulation within the street. As depicted in Figure 10, the variation in street interface density across different plans' models exhibits discernible effects on the microclimate within the street. The average wind speed demonstrates a

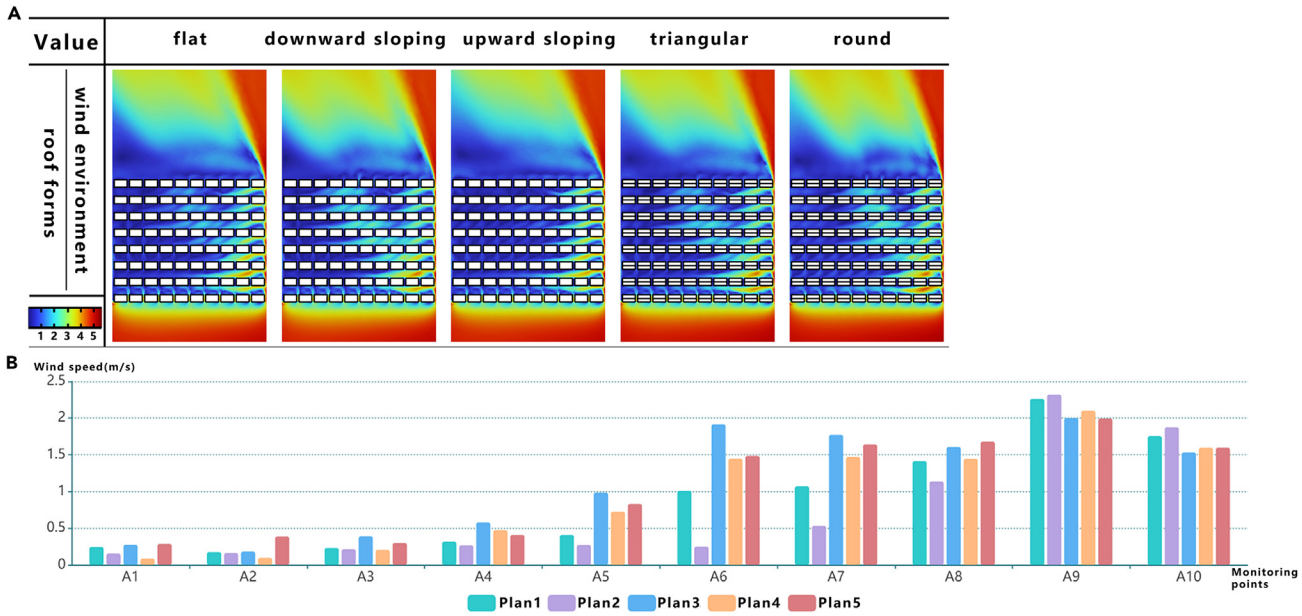

Figure 7. Simulation results of street wind environment under different roof forms parameters

(A) Visualization of the simulated street wind environment.

(B) Wind speed at each monitoring point within the street.

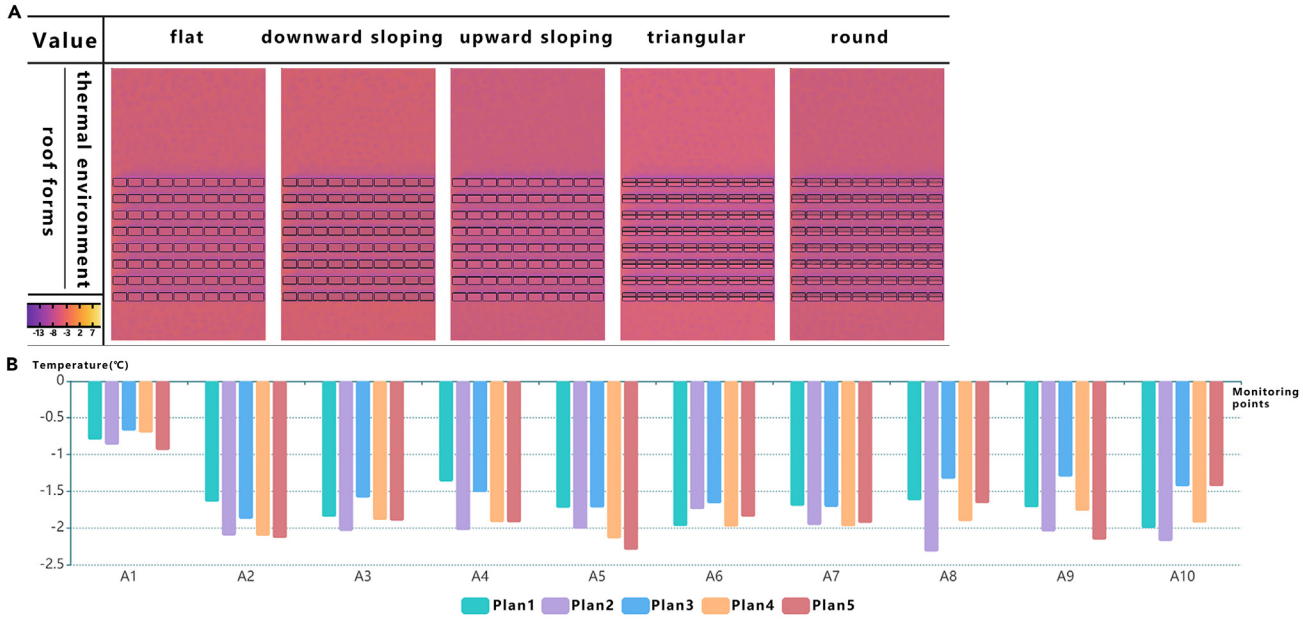

Figure 8. Simulation results of street thermal environment under different roof forms parameters

(A) Visualization of the simulated street thermal environment.

(B) Temperatures speed at each monitoring point within the street.

consistent trend of initially decreasing and then increasing values, while the average temperature follows an opposite pattern, except for plan 4. Notably, certain plans' models with specific interface densities, such as plan 6 for wind environment and plan 4 for thermal environment, exhibit significant fluctuations in both wind and thermal conditions within the street. Such fluctuations can potentially lead to reduced human comfort. Thus, when considering the interface density for urban street design, careful consideration should be given to the desired objectives. For prioritizing ventilation, either higher or lower interface densities, as exemplified in plan 1 and plan 6, may be suitable choices. Conversely, if thermal insulation is of primary concern, a moderate interface density, as demonstrated in plan 3 and plan 5, would be more preferable.

Furthermore, it is important to note that the magnitude of microclimate fluctuations within the street corresponds to the variance of the measurement point data. Higher variance values indicate larger microclimate fluctuations, which can detrimentally affect human comfort. Thus, in the pursuit of optimizing human comfort, it is advisable to avoid implementing plans 1 and 6, which exhibit larger variances.

With reference to Figure 11, the street aspect ratio has a notable influence on the microclimate within the street. An overall trend is observed, where an increase in the street aspect ratio corresponds to an increase in average wind speed, demonstrating a direct proportionality. Conversely, the average temperature exhibits an inverse relationship with the street aspect ratio, showing a decreasing trend. Furthermore, the variance in wind speed at the measurement points within the street is smaller when the aspect ratio is relatively large or small, indicating a more stable condition. However, the variance in temperature at these points increases as the aspect ratio increases, indicating that a larger aspect ratio leads to greater temperature fluctuations within the street.

In consideration of the winter season in Shenyang, it is found that reducing the street aspect ratio can effectively improve the temperature within the street, thus creating a more favorable environment for pedestrians. When designing the aspect ratio for urban streets, a larger aspect ratio may be chosen if prioritizing ventilation, while a smaller aspect ratio may be preferred for thermal insulation purposes. Moreover, the significant changes in variance observed at different aspect ratios can have a direct impact on human comfort. Therefore, for optimal human comfort, it is advisable to select a smaller aspect ratio, such as plan 1 or plan 2, when determining the street design.

The roof forms of the buildings along the street in plan 1 to plan 5 models encompass a variety of designs, including flat roofs, sloping downward roofs, sloping upward roofs, triangular roofs, and round roofs, as depicted in Figure 12. Analysis of the average wind speed and average temperature reveals notable variations among the different plans' models. Specifically, plan 3 demonstrates the highest values for both parameters, indicating a favorable wind environment and higher temperatures within the street. Conversely, plan 2 exhibits the lowest average wind speed and average temperature. These findings suggest that the roof form of the buildings plays a significant role in shaping the flow fields above the structures, consequently influencing the temperature distribution within the street. To optimize the thermal conditions during the winter season in Shenyang, the adoption of sloping upward roof designs proves effective in providing insulation within the street, thereby creating a more favorable environment for pedestrians.

Furthermore, it is worth noting that this particular roof design showcases lower variance in measurement data, which contributes to improved human comfort. By achieving a balance between ventilation and thermal insulation within the street, the sloping upward roof design demonstrates its potential to enhance the overall microclimate.

Table 1. Block spatial morphology index parameters and block spatial perception quality

Block spatial perception quality	Street conforming line ratio (B/P)	Street interface density (De)	Street aspect ratio (H/D)
Excellent	50% ≤ B/P<70%	De>70%	0.5 < H/D ≤ 1
Good	B/P>70%	50%≤De<70%	H/D ≤ 0.5
Poor	B/P<50%	De<50%	H/D > 1

The findings of this study align with Abdollahzadeh and Biloria,[40] who simulated a humid subtropical climate. They emphasized the positive impact of street conforming line ratio, interface density, and aspect ratio on outdoor thermal comfort. However, our results differ regarding the most influential factor on thermal comfort. Their study highlighted the efficiency of the street interface density factor in that climate. Additionally, their research suggested that wind velocity had the most significant impact on thermal comfort, in contrast to our findings. Similarly, Achour-Younsi and Kharrat,[41] focusing on a Mediterranean subtropical climate, concurred with our study on the importance of street conforming line ratio, interface density, and aspect ratio for thermal comfort. Furthermore, Limona et al.,[42] studying a coastal region climate, also supported the significance of street conforming line ratio and aspect ratio in enhancing thermal comfort. However, there is a discrepancy in the extent to which street conforming line ratio plays a substantial role in achieving comfort.

Indicators parameter selection and optimization strategies based on different types of streets

Based on the urban street classification provided in the "Design Guidelines for the Integration of Urban Streets in Chengdu Parks,"[43] living streets, commercial streets, and traffic-type streets are closely associated with the lives of urban residents. Living streets primarily serve as public spaces for residents to live, play, relax, and communicate, with the aim of creating a warm and comfortable street environment. When designing living streets, it is crucial to consider the microclimate within the streets, including aspects such as thermal insulation and energy efficiency, while also focusing on the spatial perception quality of the streets. By integrating spatial perception quality and the influence of microclimate, the optimal design strategy for living streets is derived, which includes a street conforming line ratio of 51.0%, a street interface density of 69.3%, a street aspect ratio of 0.88, and an upward sloping roof form for the buildings.

Commercial streets are designed to cater to diverse consumer needs, provide leisure activities, and meet experiential demands, with the objective of creating vibrant and distinctive street scenes. The design focus of commercial streets revolves around enhancing pedestrian comfort, creating pleasant dimensions for the streets, and enriching the visual aspects of the street spaces. Similar to living streets, spatial perception quality is an important consideration for commercial streets. However, commercial streets typically experience higher pedestrian flow dispersed throughout different areas of the street. Therefore, it is crucial to address the microclimate within the street by minimizing climate fluctuations and improving pedestrian comfort. In light of these considerations, the optimal design strategy for commercial streets is determined by taking into account both spatial perception quality and microclimate factors. The recommended design parameters are as follows: a street conforming line ratio of 68.0%, a street interface density of 52.0%, a street aspect ratio of 0.88 or 1.00, and a building roof form that can be either flat or upward sloping.

Traffic-type streets have the primary objective of ensuring pedestrian safety and facilitating efficient vehicular traffic, aiming to create street scenes that are efficient, safe, environmentally friendly, and convenient. Unlike living and commercial streets, traffic-type streets place less emphasis on individuals' perception of the street space and more on functional aspects. In the design of traffic-type streets, the focus shifts to the wind environment within the streets. A well-designed ventilation system plays a crucial role in reducing air pollution concentrations within the streets and enhancing the overall ventilation capacity of the city. By optimizing the wind environment, traffic-type streets can contribute to a healthier and more comfortable urban environment. Based on the results of wind environment simulations conducted for

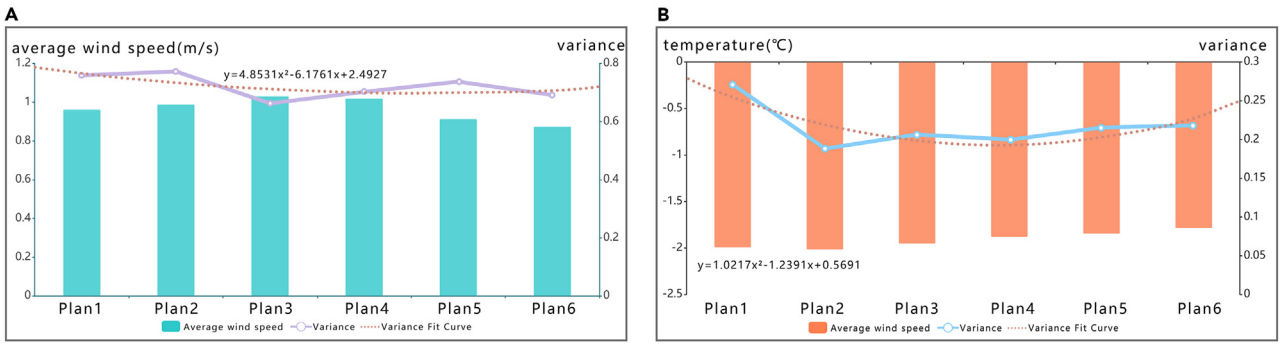

Figure 9. Microclimate analysis under street conforming line ratio

(A) The analysis of wind environment simulation results.

(B) The analysis of thermal environment simulation results.

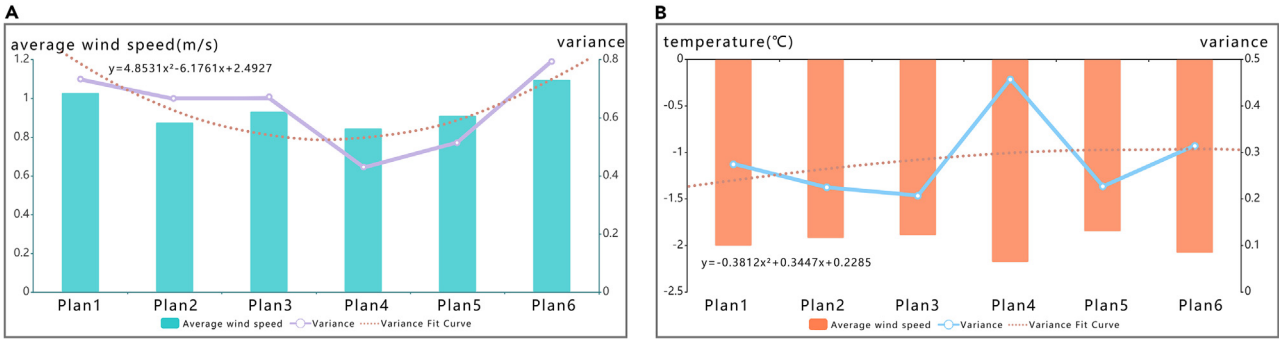

Figure 10. Microclimate analysis under street interface density

(A) The analysis of wind environment simulation results.

(B) The analysis of thermal environment simulation results.

the streets, the optimal design parameters for traffic-type streets include a street conforming line ratio of 68.0%, a street interface density of 43.3%, a street aspect ratio of 1.63, and a building roof form that can be upward sloping.

Considering the importance of these findings, we suggest precise design strategies customized for various types of urban streets, which have a direct influence on residents' quality of life (Table 2).

Limitations of the study

This study primarily focuses on exploring the impact of four morphological indicators related to the form of block public spaces (street conforming line ratio, street interface density, street aspect ratio, and building roof forms) on the microclimate of block streets. These four indicators are mainly associated with the buildings along the streets, while other elements of the block, such as road surfaces and paving, landscape greenery, and public spaces, have not been comprehensively considered. In the simulation analysis of the street aspect ratio, the numerical model varies the height of the buildings on both sides while keeping the street width constant to increase the street aspect ratio. However, in real life, different grades of roads correspond to different road widths, and the influence of street aspect ratio under different road widths on the microclimate of the street has not been considered.

In conclusion, due to the limited number of case studies discussed in this research, future studies should conduct more simulation analyses and field measurements under different parameter conditions, supplementing and validating the existing research findings. This will provide more comprehensive guidance for the planning and layout of block spatial morphologies.

Conclusion

In this study, we delved into the intricate relationship between various morphological indicators and the microclimate of urban block streets. Through extensive numerical simulations and a consideration of human perception within these urban spaces, we arrived at several noteworthy findings that bear substantial implications for urban design and environmental quality enhancement.

1. Street conforming line ratio: We observed that as the street conforming line ratio decreases, there is an initial increase in average wind speed within the street, followed by a subsequent decrease. This reduction in street conforming line ratio is also accompanied by a gradual rise in average temperature.

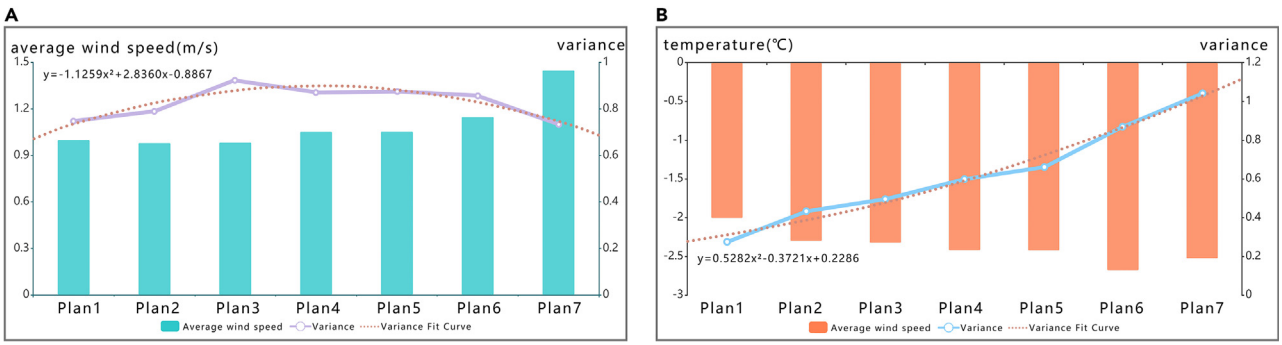

Figure 11. Microclimate analysis under street aspect ratio

(A) The analysis of wind environment simulation results; (B) The analysis of thermal environment simulation results.

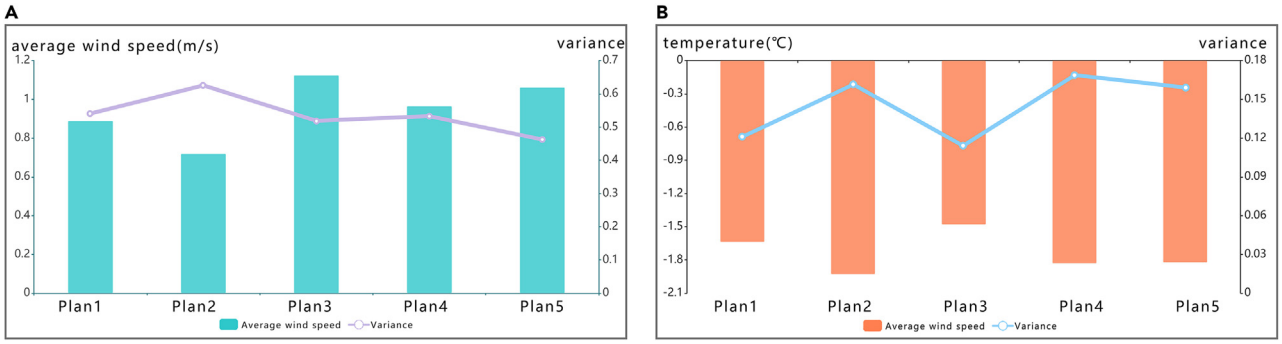

Figure 12. Microclimate analysis under roof forms

(A) The analysis of wind environment simulation results.

(B) The analysis of thermal environment simulation results.

2. Street interface density: Decreasing the street interface density initially reduces average wind speed within the street, only to later increase it. Paradoxically, the average temperature follows an opposite trend, showing a decrease when the average wind speed is high and vice versa.
3. Street aspect ratio: Our study revealed that an increase in street aspect ratio leads to a proportional increase in average wind speed, while inversely causing a decrease in average temperature within the street.
4. Building roof forms: Roof forms played a significant role in microclimate variation. Streets lined with upward sloping roofs exhibited the highest average wind speed and temperature, while streets featuring downward sloping roofs had the lowest values.

By combining the results of numerical simulations on street microclimate with people's perception of the block space, this study offers a comprehensive approach for evaluating urban block microclimates. In the meantime, we propose spatial layout design strategies suitable for different types of streets (i.e., living streets, commercial streets, and traffic-type streets) in severe cold regions, taking into account the climate environment. While our study was conducted in Shenyang, China, the principles and insights gleaned can be extended to different climatic zones to optimize the spatial layout of urban blocks across diverse regions. In summary, this study offers valuable insights into the interplay between morphological indicators and microclimates within urban block streets. Future research endeavors should explore a range of geographic contexts, expand the scope of microclimate evaluation, and continue to refine evaluation criteria, ultimately advancing our understanding and application of urban block spatial layout principles.

STAR★METHODS

Detailed methods are provided in the online version of this paper and include the following:

- KEY RESOURCES TABLE
- RESOURCE AVAILABILITY
  - Lead contact
  - Materials availability
  - Data and code availability
- METHODS DETAILS
  - Study area overview
  - Numerical model construction
  - Master control equations

SUPPLEMENTAL INFORMATION

Supplemental information can be found online at https://doi.org/10.1016/j.isci.2023.108313.

Table 2. Customized design strategies for various types of urban streets

Street type	Street conforming line ratio	Street interface density	Street aspect ratio	Building roof forms
Residential streets	51.0%	69.3%	0.88	Upward sloping
Commercial streets	68.0%	52.0%	0.88 or 1.00	Flat or upward sloping
Traffic-oriented streets	68.0%	43.3%	1.63	Upward sloping

ACKNOWLEDGMENTS

This research was funded by the National Natural Science Foundation of China (Nos. 32101325 and 41871162), the Liaoning Provincial Natural Science Foundation of China (No. 2023-MS-084), and the Fundamental Research Funds for the Central Universities (No. N2211001).

AUTHOR CONTRIBUTIONS

Conceptualization, G.Z., Y.C., and W.W.; formal analyses, G.Z., Y.C., W.W., Y.T., and R.L.; investigation, G.Z., Y.T., and P.L.; writing – original draft, G.Z., Y.C., W.W., Y.T., A.X., and R.L.; writing – review and editing, all authors have read, edited, and approved the manuscript; visualization, G.Z. and Y.C.; funding acquisition, W.W.

DECLARATION OF INTERESTS

The authors declare no competing interests.

INCLUSION AND DIVERSITY

We support inclusive, diverse, and equitable conduct of research.

Received: June 20, 2023
Revised: September 6, 2023
Accepted: October 20, 2023
Published: October 23, 2023

REFERENCES

1. Cao, Q., Luan, Q., Liu, Y., and Wang, R. (2021). The effects of 2D and 3D building morphology on urban environments: A multi-scale analysis in the Beijing metropolitan region. Build. Environ. *192*, 107635. https://doi.org/10.1016/j.buildenv.2021.107635.
2. Liu, X., Hu, G., Chen, Y., Li, X., Xu, X., Li, S., Pei, F., and Wang, S. (2018). High-resolution multi-temporal mapping of global urban land using Landsat images based on the Google Earth Engine Platform. Remote Sens. Environ. *209*, 227–239. https://doi.org/10.1016/j.rse.2018.02.055.
3. Chan, S.Y., and Chau, C.K. (2019). Development of artificial neural network models for predicting thermal comfort evaluation in urban parks in summer and winter. Build. Environ. *164*, 106364. https://doi.org/10.1016/j.buildenv.2019.106364.
4. Buyantuyev, A., and Wu, J. (2010). Urban heat islands and landscape heterogeneity: linking spatiotemporal variations in surface temperatures to land-cover and socioeconomic patterns. Landsc. Ecol. *25*, 17–33. https://doi.org/10.1007/s10980-009-9402-4.
5. Cao, Q., Yu, D., Georgescu, M., Wu, J., and Wang, W. (2018). Impacts of future urban expansion on summer climate and heat-related human health in eastern China. Environ. Int. *112*, 134–146. https://doi.org/10.1016/j.envint.2017.12.027.
6. Georgescu, M. (2015). Challenges Associated with Adaptation to Future Urban Expansion. J. Clim. *28*, 2544–2563. https://doi.org/10.1175/JCLI-D-14-00290.1.
7. Konstantinov, P., Varentsov, M., and Esau, I. (2018). A high density urban temperature network deployed in several cities of Eurasian Arctic. Environ. Res. Lett. *13*, 075007. https://doi.org/10.1088/1748-9326/aacb84.
8. Demuzere, M., Orru, K., Heidrich, O., Olazabal, E., Geneletti, D., Orru, H., Bhave, A.G., Mittal, N., Feliu, E., and Faehnle, M. (2014). Mitigating and adapting to climate change: Multi-functional and multi-scale assessment of green urban infrastructure. J. Environ. Manage. *146*, 107–115. https://doi.org/10.1016/j.jenvman.2014.07.025.
9. Su, H., Han, G., Li, L., and Qin, H. (2021). The impact of macro-scale urban form on land surface temperature: An empirical study based on climate zone, urban size and industrial structure in China. Sustain. Cities Soc. *74*, 103217. https://doi.org/10.1016/j.scs.2021.103217.
10. Yang, J., Zhan, Y., Xiao, X., Xia, J.C., Sun, W., and Li, X. (2020). Investigating the diversity of land surface temperature characteristics in different scale cities based on local climate zones. Urban Clim. *34*, 100700. https://doi.org/10.1016/j.uclim.2020.100700.
11. Yang, J., Ren, J., Sun, D., Xiao, X., Xia, J.C., Jin, C., Li, X., and Li, X. (2021). Understanding land surface temperature impact factors based on local climate zones. Sustain. Cities Soc. *69*, 102818. https://doi.org/10.1016/j.scs.2021.102818.
12. He, M., Li, W., Wang, P., and Yao, C. (2022). Allocation equity of regulating ecosystem services from blue-green infrastructures: A case study of street blocks in Wuhan central city. Ecol. Indic. *138*, 108853. https://doi.org/10.1016/j.ecolind.2022.108853.
13. Kang, J., Li, C., Zhang, B., Zhang, J., Li, M., and Hu, Y. (2023). How do natural and human factors influence ecosystem services changing? A case study in two most developed regions of China. Ecol. Indic. *146*, 109891. https://doi.org/10.1016/j.ecolind.2023.109891.
14. Li, F., Zhou, T., and Lan, F. (2021). Relationships between urban form and air quality at different spatial scales: A case study from northern China. Ecol. Indic. *121*, 107029. https://doi.org/10.1016/j.ecolind.2020.107029.
15. Tse, K.T., Weerasuriya, A.U., and Kwok, K.C.S. (2016). Simulation of twisted wind flows in a boundary layer wind tunnel for pedestrian-level wind tunnel tests. J. Wind Eng. Ind. Aerodyn. *159*, 99–109. https://doi.org/10.1016/j.jweia.2016.10.010.
16. Zhang, M., and Gao, Z. (2021). Effect of urban form on microclimate and energy loads: Case study of generic residential district prototypes in Nanjing, China. Sustain. Cities Soc. *70*, 102930. https://doi.org/10.1016/j.scs.2021.102930.
17. Sharmin, T., Steemers, K., and Matzarakis, A. (2017). Microclimatic modelling in assessing the impact of urban geometry on urban thermal environment. Sustain. Cities Soc. *34*, 293–308. https://doi.org/10.1016/j.scs.2017.07.006.
18. Yan, H., Fan, S., Guo, C., Wu, F., Zhang, N., and Dong, L. (2014). Assessing the effects of landscape design parameters on intra-urban air temperature variability: The case of Beijing, China. Build. Environ. Times *76*, 44–53. https://doi.org/10.1016/j.buildenv.2014.03.007.
19. Jamei, E., and Rajagopalan, P. (2017). Urban development and pedestrian thermal comfort in Melbourne. Sol. Energy *144*, 681–698. https://doi.org/10.1016/j.solener.2017.01.023.
20. Ma, T., and Chen, T. (2022). Outdoor ventilation evaluation and optimization based on spatial morphology analysis in Macau. Urban Clim. *46*, 101335. https://doi.org/10.1016/j.uclim.2022.101335.
21. Mei, S.-J., Hu, J.-T., Liu, D., Zhao, F.-Y., Li, Y., Wang, Y., and Wang, H.-Q. (2017). Wind driven natural ventilation in the idealized building block arrays with multiple urban morphologies and unique package building density. Energy Build. *155*, 324–338. https://doi.org/10.1016/j.enbuild.2017.09.019.
22. Ng, E., Yuan, C., Chen, L., Ren, C., and Fung, J.C.H. (2011). Improving the wind environment in high-density cities by understanding urban morphology and surface roughness: A study in Hong Kong. Landsc. Urban Plan. *101*, 59–74. https://doi.org/10.1016/j.landurbplan.2011.01.004.
23. Chen, L., DiPietro, L.A., Sandberg, M., Claesson, L., Di Sabatino, S., and Wigo, H. (2017). The impacts of building height variations and building packing densities on

flow adjustment and city breathability in idealized urban models. Adv. Wound Care *6*, 344–355. https://doi.org/10.1016/j.buildenv.2017.03.042.

24. Chew, L.W., and Norford, L.K. (2019). Pedestrian-level wind speed enhancement with void decks in three-dimensional urban street canyons. Build. Environ. *155*, 399–407. https://doi.org/10.1016/j.buildenv.2019.03.058.
25. Zhang, Y., Ou, C., Chen, L., Wu, L., Liu, J., Wang, X., Lin, H., Gao, P., and Hang, J. (2020). Numerical studies of passive and reactive pollutant dispersion in high-density urban models with various building densities and height variations. Build. Environ. *177*, 106916. https://doi.org/10.1016/j.buildenv.2020.106916.
26. Li, Y., and Chen, L. (2020). Study on the influence of voids on high-rise building on the wind environment. Build. Simul. *13*, 419–438. https://doi.org/10.1007/s12273-019-0584-7.
27. Liu, Z., Yu, Z., Chen, X., Cao, R., and Zhu, F. (2020). An investigation on external airflow around low-rise building with various roof types: PIV measurements and LES simulations. Build. Environ. *169*, 106583. https://doi.org/10.1016/j.buildenv.2019.106583.
28. Llaguno-Munitxa, M., Bou-Zeid, E., and Hultmark, M. (2017). The influence of building geometry on street canyon air flow: Validation of large eddy simulations against wind tunnel experiments. J. Wind Eng. Ind. Aerodyn. *165*, 115–130. https://doi.org/10.1016/j.jweia.2017.03.007.
29. Xu, X., Yang, Q., Yoshida, A., and Tamura, Y. (2017). Characteristics of pedestrian-level wind around super-tall buildings with various configurations. J. Wind Eng. Ind. Aerodyn. *166*, 61–73. https://doi.org/10.1016/j.jweia.2017.03.013.
30. Zhang, X., Zhou, Y., Yang, J., Wang, Y., Yang, W., Gao, L., Xiang, Y., and Zhang, F. (2020). Pedestrian-level wind environment near a super-tall building with unconventional configurations in a regular urban area. Build. Simul. *20*, 439–456. https://doi.org/10.1007/s12273-019-0588-3.
31. Peng, Y., Gao, Z., Buccolieri, R., Shen, J., and Ding, W. (2021). Urban ventilation of typical residential streets and impact of building form variation. Sustain. Cities Soc. *67*, 102735. https://doi.org/10.1016/j.scs.2021.102735.
32. Zhang, A., Xia, C., and Li, W. (2022). Relationships between 3D urban form and ground-level fine particulate matter at street block level: Evidence from fifteen metropolises in China. Build. Environ. *211*, 108745. https://doi.org/10.1016/j.buildenv.2021.108745.
33. Liu, X., Zeng, S., Namaiti, A., and Xin, R. (2023). Comparison between three convolutional neural networks for local climate zone classification using Google Earth Images: A case study of the Fujian Delta in China. Ecol. Indic. *148*, 110086. https://doi.org/10.1016/j.ecolind.2023.110086.
34. Shen, Z.-J., Zhang, B.-H., Xin, R.-H., and Liu, J.-Y. (2022). Examining supply and demand of cooling effect of blue and green spaces in mitigating urban heat island effects: A case study of the Fujian Delta urban agglomeration (FDUA), China. Ecol. Indic. *142*, 109187. https://doi.org/10.1016/j.ecolind.2022.109187.
35. Lynch, K. (1960). The Image of the City (MIT Press). https://www.miguelangelmartinez.net/IMG/pdf/1960_Kevin_Lynch_The_Image_of_The_City_book.pdf.
36. Pang, J., Fan, Z., Yang, M., Liu, J., Zhang, R., Wang, W., and Sun, L. (2023). Effects of complex spatial atrium geometric parameters on the energy performance of hotels in a cold climate zone in China. J. Build. Eng. *72*, 106698. https://doi.org/10.1016/j.jobe.2023.106698.
37. Jacobs, A.B. (1995). Great Streets (The MIT Press). https://mitpress.mit.edu/9780262600231/great-streets/.
38. Sitte, C. (1945). The Art of Building Cities. https://www.jstor.org/stable/40101896.
39. Jacobs, J. (1992). The Death and Life of Great American Cities (Vintage). https://smartnet.niua.org/sites/default/files/resources/The%20Importance%20of%20Dealth%20and%20Life%20Final.pdf.
40. Abdollahzadeh, N., and Biloria, N. (2021). Outdoor thermal comfort: Analyzing the impact of urban configurations on the thermal performance of street canyons in the humid subtropical climate of Sydney. Front. Archit. Res. *10*, 394–409. https://doi.org/10.1016/j.foar.2020.11.006.
41. Achour-Younsi, S., and Kharrat, F. (2016). Outdoor Thermal Comfort: Impact of the Geometry of an Urban Street Canyon in a Mediterranean Subtropical Climate – Case Study Tunis, Tunisia. Procedia - Soc. Behav. Sci. *216*, 689–700. https://doi.org/10.1016/j.sbspro.2015.12.062.
42. Iimona, S.S., Al-hagla, K.S., and El-sayad, Z.T. (2019). Using simulation methods to investigate the impact of urban form on human comfort. Case study: Coast of Baltim, North Coast, Egypt. Alex. Eng. J. *58*, 273–282. https://doi.org/10.1016/j.aej.2019.02.002.
43. Chengdu Municipal Bureau of Planning and Natural Resources (2020). Guidelines for the Integrated Design of Streets in Park City Chengdu. http://mpnr.chengdu.gov.cn/ghhzrzyj/sjwj/2020-07/07/content_4abd7e9a64dd4deba9d30e8102c18eec.shtml.
44. MOHURD (2016). Code for Thermal Design of Civil Building (GB 50176-2016). Ministry of Housing and Urban-Rural Development of the People Republic of China: Beijing. https://www.chinesestandard.net/PDF/English.aspx/GB50176-2016.
45. He, X., Gao, W., Wang, R., and Yan, D. (2023). Study on outdoor thermal comfort of factory areas during winter in hot summer and cold winter zone of China. Build. Environ. *228*, 109883. https://doi.org/10.1016/j.buildenv.2022.109883.
46. Yin, Q., Cao, Y., and Sun, C. (2021). Research on outdoor thermal comfort of high-density urban center in severe cold area. Build. Environ. *200*, 107938. https://doi.org/10.1016/j.buildenv.2021.107938.
47. Alkhoudiri, A., Navarro, I., Fort, J.M., and Alumran, S. (2022). Parametric comparative analysis of outdoor thermal comfort in a desert climate: A case study of single-family houses in Riyadh. Urban Clim. *46*, 101300. https://doi.org/10.1016/j.uclim.2022.101300.
48. Li, J., Wang, Y., and Xia, Y. (2022). A novel geometric parameter to evaluate the effects of block form on solar radiation towards sustainable urban design. Sustain. Cities Soc. *84*, 104001. https://doi.org/10.1016/j.scs.2022.104001.
49. Kuang, X., and Xu, W. (2012). Urban Planning Management Based Street Facade Control Methods. Planners *28*, 70–75. https://kns.cnki.net/kcms2/article/abstract?v=mFW-2yKNQdqRSQCtDEWH2NLVQyf5Xo3p2XDUx7Rue-oyZoIT8K_XqXCtCgI-XgGKp0tMzSlu5QEtYNao5pzkN_Au2Fr3yjPmPKuRn8bQf70k8XNe1cupMEjSS6jUHofq&uniplatform=NZKPT&language=CHS.
50. Liu, M., Wei, D., and Chen, H. (2022). Consistency of the relationship between air pollution and the urban form: Evidence from the COVID-19 natural experiment. Sustain. Cities Soc. *83*, 103972. https://doi.org/10.1016/j.scs.2022.103972.
51. Deng, J.-Y., and Wong, N.H. (2020). Impact of urban canyon geometries on outdoor thermal comfort in central business districts. Sustain. Cities Soc. *53*, 101966. https://doi.org/10.1016/j.scs.2019.101966.
52. Allegrini, J. (2018). A wind tunnel study on three-dimensional buoyant flows in street canyons with different roof shapes and building lengths. Build. Environ. *143*, 71–88. https://doi.org/10.1016/j.buildenv.2018.06.056.
53. Shaeri, J., Mahdavinejad, M., and Pourghasemian, M.H. (2022). A new design to create natural ventilation in buildings: Wind chimney. J. Build. Eng. *59*, 105041. https://doi.org/10.1016/j.jobe.2022.105041.
54. Ascione, F., Bianco, N., De Stasio, C., Mauro, G.M., and Vanoli, G.P. (2015). Dynamic insulation of the building envelope: Numerical modeling under transient conditions and coupling with nocturnal free cooling. Appl. Therm. Eng. *84*, 1–14. https://doi.org/10.1016/j.applthermaleng.2015.03.039.
55. Meng, D., Dang, X., Wang, A., and Zhao, W. (2023). Optimization of double-layer shaped phase change wallboard in buildings in two typical climate areas in China. J. Energy Storage *61*, 106698. https://doi.org/10.1016/j.est.2023.106698.
56. Yang, X., Almojil, S.F., Yang, Y., Almohana, A.I., Alali, A.F., Rajhi, A.A., Alamri, S., Qasim, F., Ren, Y., Zhang, Z., et al. (2022). The effect of using phase change materials in the walls of a building on the amount of carbon dioxide production and reducing fuel consumption. J. Build. Eng. *59*, 105058. https://doi.org/10.1016/j.jobe.2022.105058.
57. Jha, A., and Tripathy, P.P. (2019). Heat transfer modeling and performance evaluation of photovoltaic system in different seasonal and climatic conditions. Renew. Energy *135*, 856–865. https://doi.org/10.1016/j.renene.2018.12.032.
58. Wang, W., Cheng, X., and Dai, M. (2022). Strategies for sustainable urban development and morphological optimization of street canyons: Measurement and simulation of PM2.5 at different points and heights. Sustain. Cities Soc. *87*, 104191. https://doi.org/10.1016/j.scs.2022.104191.

STAR★METHODS

KEY RESOURCES TABLE

REAGENT or RESOURCE	SOURCE	IDENTIFIER
Software and algorithms		
Graph Plotting	Origin Lab	https://www.originlab.com/index.aspx?go=PRODUCTS/Origin
Computational Fluid Dynamics (CFD) model	COMSOL Multiphysics Software	https://www.comsol.com/comsol-multiphysics
Radiation (RAD) model	COMSOL Multiphysics Software	https://www.comsol.com/comsol-multiphysics
Other		
Meteorological data	National Climatic Data Center	https://www.ncei.noaa.gov/

RESOURCE AVAILABILITY

Lead contact

Further information and requests for resources should be directed to and will be fulfilled by the lead contact, Wen Wu (wuwen@mail.neu.edu.cn).

Materials availability

This study did not generate new unique materials.

Data and code availability

Any additional information required to reanalyze the data reported in this paper is available from the lead contact upon request.

METHODS DETAILS

Study area overview

Based on the " Code for thermal design of civil building" (GB 50176–2016),[44] China is categorized into five thermal climate zones determined by factors such as temperature, relative humidity, and precipitation. These zones encompass: severe cold, cold, cold-winter and hot-summer, warm-winter and hot-summer, and warm climate zones. This classification is also applicable for characterizing urban climates.[45,46] Buildings situated in different thermal climate zones may necessitate distinct spatial morphologies and orientations to effectively respond to their respective local climates (Table S1). Consequently, in our study focusing on the influence of urban block spatial morphology in the cold region of Shenyang, we have taken into consideration the criteria for cold regions as outlined in the "Code for thermal design of civil building" (GB 50176-2016). The severe cold region exhibits specific climatic characteristics, including a short and windy spring with sandstorms, a brief and cool summer, a long and dry autumn with notable temperature fluctuations between morning/evening and other times, an extended and cold winter marked by prolonged freezing periods and heavy snow cover, abundant sunshine, high solar radiation, and strong winter winds.

Shenyang (41°11′51″–43°02′13″N, 122°25′09″–123°48′24″E) falls within the severe cold region according to the climate classification. It experiences a temperate continental climate with distinct four seasons and is situated in the southern part of Northeast China, in the central region of Liaoning Province. Analysis of meteorological data from the National Climatic Data Center (https://www.ncei.noaa.gov/) spanning the past five years (2018–2022) reveals that the prevailing wind direction in Shenyang during winter is southeast-south (SSE), with a high frequency of 17%. The average winter wind speed is 3.8 m/s, reaching a maximum speed of 8 m/s. The average winter temperature in Shenyang over the past five years is −10.23°C, with an average maximum temperature of −4.27°C and an average minimum temperature of −16.18°C (Figure S1). In general, Shenyang experiences severe cold temperatures, strong winter winds, and a dry climate during winter.

Numerical model construction

The microclimate of urban blocks is influenced by various factors, including the geometric form, layout, parameters, and local climatic conditions of street canyons. These street canyon characteristics encompass indicators such as street conforming line ratio, interface density, aspect ratio, scale, orientation, openness, sky view factor (SVF), network line density, and architectural roof forms.[36,47,48]

In this study, four morphological indicators closely associated with the spatial of urban blocks were selected: street conforming line ratio, street interface density, street aspect ratio, and building roof forms. These indicators were utilized in the construction of a numerical model to simulate the urban blocks. The model included eight idealized streets, where the width of the street canyon (D) was kept constant at 24m. The buildings within the model had a floor height of 3m and maintained a consistent roof height (L) of 3m. For instance, in the case of a flat-roofed building, the building height (H) was set to 21m. To account for ground effects, a ground layer of 2.5m was introduced in the model, comprising a 0.7m asphalt surface and a 1.8m soil layer. The overall dimensions of the numerical simulation domain were

748 m × 412 m × 170.5m. The study area was defined as the region between the fourth and fifth buildings, and ten measurement points (A1-A10) were evenly distributed along the centerline of the street (Figure S2).

The objective of this study was to investigate the influence of street spatial morphology on the microclimate within street canyons of urban blocks using a numerical model. To achieve this, specific common features were selected from the complex spatial morphologies observed in real-world blocks, following the principles of selecting the "most representative and frequently occurring street block morphology" and ensuring "diversity in patterns for convenient single-factor comparative studies." A total of 24 cases were generated based on the four morphological indicators: street conforming line ratio, interface density, aspect ratio, and building roof forms (Figure S3).

Conforming Line Ratio: It is defined as the ratio of the total length of building facades directly adjacent to the street's defined building line to the length of the building control line. The conforming line ratio is a crucial metric used to assess the continuity of street spaces. A higher ratio corresponds to a neater visual appearance along the street.[49] Interface Density: Interface density refers to the ratio of the combined width of building facades projecting onto one side of the street to the length of that street segment. Interface density is influenced by the number of enclosing buildings along a street and is interconnected with block-level building density. Continuous street interfaces can be disrupted by transverse streets, impacting interface density.[50] Aspect Ratio: The aspect ratio of streets is a factor characterizing the spatial form of streets. It represents the ratio of the heights of buildings on both sides of a street to the width of that street. This ratio depends on the street width and the heights of buildings on either side. Different values of street aspect ratio reflect various spatial features and visual effects.[51] Building Roof Forms: Building roof forms describe the geometric shapes of building roofs, such as flat, sloped, or round roofs.[52] These forms play a pivotal role in shaping urban skylines and the visual characteristics of buildings. The parameter settings for each case are presented in Table S2.

Master control equations

The numerical simulation model employed in this study incorporates two integrated sub-models within COMSOL Multiphysics 6.0. The first sub-model is the Computational Fluid Dynamics (CFD) model, which resolves the convection heat transfer between the air, building surfaces, and the ground.[53] The second sub-model is the radiation (RAD) model, which computes the shortwave and longwave radiation exchanges between the building surfaces, the ground, and the sky.[54,55] The CFD model adopts the Reynolds averaging method to solve the Navier-Stokes equations, considering thermal effects and employing the Boussinesq approximation, assuming that fluid density varies solely with temperature. For incompressible fluids, the master control equations encompass the following three equations: continuity equation (Equation 1), conservation of momentum equation (Equation 2), energy conservation equation (Equation 3) are as follows:

$$\frac{\partial \overline{u_i}}{\partial x_i} = 0 \qquad \text{(Equation 1)}$$

$$\overline{u_j}\frac{\partial \overline{u_i}}{\partial \overline{x_j}} = -\frac{1}{\rho}\frac{\partial \overline{P}}{\partial x_i} + \frac{v}{\rho}\frac{\partial^2 \overline{u_i}}{\partial x_i \partial x_j} - \frac{\partial}{\partial x_j}\left(\overline{u_i u_j}\right) + f_i \qquad \text{(Equation 2)}$$

$$\overline{u_i}\frac{\partial \overline{T}}{\partial x_i} + \frac{\partial}{\partial x_i}\left(K_T \frac{\partial \overline{T}}{\partial x_i}\right) = 0 \qquad \text{(Equation 3)}$$

In the given equations: x_i represents the spatial coordinates, $\overline{u_i}$ denotes the average fluid velocity, $\overline{u_i u_j}$ represents the Reynolds stress, $\overline{P}$ represents the pressure, ρ represents the air density, v is the dynamic viscosity, f_i represents the buoyancy force caused by thermal effects, $\overline{T}$ represents the potential temperature, K_T is the heat transfer coefficient.

In the context of simulating the urban wind thermal environment using COMSOL software, the synergy between the RAD and CFD models is pivotal for achieving a comprehensive understanding of heat transfer processes within a city block. The RAD model serves as the foundational component for computing radiative heat flux, which serves as a critical input for the CFD model. The CFD model, on the other hand, governs the equilibrium between temperature and fluid velocity fields, thereby influencing the distribution of heat throughout the simulated urban space. This interaction between the RAD and CFD models operates iteratively, continually refining the temperature and heat flux calculations until convergence is reached. This iterative approach ensures a consistent and balanced representation of the intricate interplay between radiation and fluid dynamics. Consequently, the coupled RAD and CFD models not only facilitate the exchange of information but also enable the accurate capture of the coupled effects of radiation and fluid flow within the urban environment. Ultimately, this iterative process results in a solution that effectively accounts for the intricate and dynamic relationship between radiative and convective heat transfer phenomena, enhancing our ability to model and understand the thermal behavior of urban areas.[56]

To enhance the model's alignment with real environmental conditions within COMSOL Multiphysics 6.0, the radiation source was designated as the sun, leveraging the software's integrated functions and tools. Key parameters, including the geographical coordinates of Shenyang (41°11′51″-43°02′13″ N, 122°25′09″-123°48′ 24″E) and the date of January 1, 2020, were employed to calculate the solar radiation angles.[57] Furthermore, the solar radiation intensity was selected as the maximum value among the hourly average radiation intensities recorded in January 2020, specifically, 550 W/m^2 at 12:00 noon.[58] To accurately emulate the actual environmental temperature conditions throughout the model's simulation, the choice was made to utilize a cosine function. This mathematical function effectively captures the temporal variations in environmental temperature. Within this framework, the average temperature observed in January 2020 serves as the

baseline temperature, while the temperature differential between the highest and lowest values recorded during that month acts as the offset parameter. Notably, the function exhibits a 24-h period to encompass daily temperature fluctuations. In the context of simulating the wind environment, a meticulous approach was applied to ensure greater representativeness. Consideration was given to the predominant wind direction experienced in Shenyang during the winter season, and the average wind speed for January in winter was thoughtfully incorporated.[53] These measures collectively contribute to the comprehensive representation of local climate conditions in our simulation results.